Proceedings Seventh Workshop Geothermal Reservoir Engineering
Stanford, December 1981. SGP-TR-55.

COLD WATER INJECTION INTO TWO-PHASE GEOTHERMAL RESERVOIRS

S. K. Garg and J. W. Pritchett

Systems, Science and Software (S^3)
P. O. Box 1620
La Jolla, California 92038

A geothermal reservoir simulator (CHARGR) is employed in its one-dimensional radial mode to examine the response of geothermal reservoirs to cold water injection from a single well. The numerical solutions are analyzed to generate interpretation techniques for pressure transient data during injection and subsequent well shutin. It is shown that the pressure buildup (i.e., injection) data may be analyzed in a straightforward manner to yield the absolute formation permeability; the pressure fall-off (i.e. shutin) data, on the other hand, appear to be of lesser utility.

Introduction Recently Garg [1980], Grant [1978], Moench and Atkinson [1977] and Sorey, et al. [1980] have examined the drawdown and buildup response of initially two-phase geothermal reservoirs. The plot of pressure drop versus logarithm of time (for drawdown test; for buildup Δp versus log $t+\Delta t/\Delta t$ should be plotted) asymptotes to a straight line after an initial non-linear period; the slope m of the straight line can be used to infer the kinematic mobility. For two-phase geothermal reservoirs, however, it is not possible to obtain the absolute formation permeability from conventional drawdown/buildup tests. If absolute formation permeability is desired, it is necessary to conduct an injection test.

At the present time, theoretical analyses of pressure injection/fall-off data are unavailable in the published literature. In the present paper, we employ a numerical reservoir simulator (CHARGR; Pritchett [1980]) to examine the response of two-phase geothermal reservoirs during cold water injection.

An examination of the numerical simulations shows that the pressure injection data may be analyzed in the conventional manner to yield absolute formation permeability. The pressure fall-off response, on the other hand, is very complex and is seen to be of limited utility in evaluating formation properties.

Numerical Examples To examine the response of a geothermal reservoir under cold water injection, the CHARGR reservoir simulator was exercised in its one-dimensional radial mode. The radially infinite reservoir was simulated using a 60-zone [Δr_1 = 0.11 m; Δr_2 = 1.2 Δr_1; Δr_3 = 1.2 Δr_2, ..., Δr_{60} = 1.2 Δr_{59}] radial grid. The outer radius of the grid is 25,825 m and is sufficiently large such that no signal reaches this boundary during the test period. The formation thickness is H = 250 m. The well is assumed to be coincident with Zone 1. (In the CHARGR code, a well can be represented as an integral part of the grid by assigning to the well-block sufficiently high permeability and porosity.) The reservoir rock is assumed to be a typical sandstone. The relevant rock properties are given in Table 1. The mixture (rock/fluid) thermal conductivity is approximated by Budiansky's formula (Pritchett [1980]). In this paper, considerations of skin effect and well storage have been ignored. These effects, while important in practical well testing, are not germane to the present discussion.

Table 1
ROCK PROPERTIES EMPLOYED IN NUMERICAL SIMULATIONS

	Rock Matrix ($2 \le i \le 60$)
Porosity, ϕ	0.1
Permeability, k(m^2)	5×10^{-14}
Uniaxial Formation Compressibility, C_m(MPa^{-1})	0
Rock Grain Density, ρ_r(kg/m^3)	2650
Grain Thermal Conductivity, K_r(W/m-°C)	5.25
Heat Capacity, c_r(kJ/kg°C)	1
Relative Permeability, ($k_{r\ell}$, k_{rg})	Corey*
Residual Liquid Saturation, $S_{\ell r}$	0.3
Residual Gas Saturation, S_{gr}	0.05

* $k_{r\ell} = (S^*_\ell)^4$, $k_{rg} = (1-S^{*2}_\ell)(1-S^*_\ell)^2$, $S^*_\ell = (S_\ell - S_{\ell r})/(1-S_{\ell r}-S_{gr})$, $S_\ell (S_g)$ = liquid (gas) volume fraction.

The initial fluid state for the two cases considered in the following is given in Table 2. The cold water is injected at a constant rate of 35 kg/s for $t = 5.868 \times 10^5$ s; the well is then shut in for $\Delta t = 1.3932 \times 10^6$ s.

Table 2
INITIAL FLUID STATE FOR COLD WATER INJECTION INTO TWO-PHASE RESERVOIRS

Case No.	Pressure MPa	Temperature °C	Steam Sat.
1	8.5917 MPa	300	0.28
2	8.5917 MPa	300	0.05

Pressure Injection Data The pressure build-up (injection) data (Figures 1 and 2) closely fit straight lines with identical slopes. The slope implies a flowing kinematic viscosity of 2.02×10^{-7} m^2/s which is in good agreement with the kinematic viscosity of the cold injected water

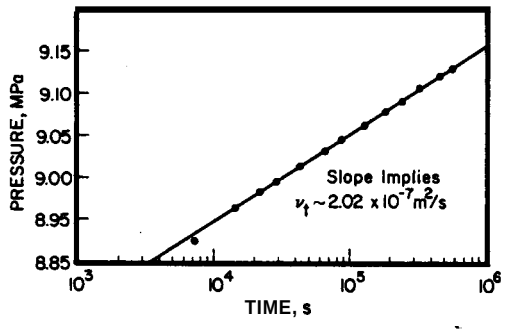

Figure 1 Pressure Injection Data for Case 1.

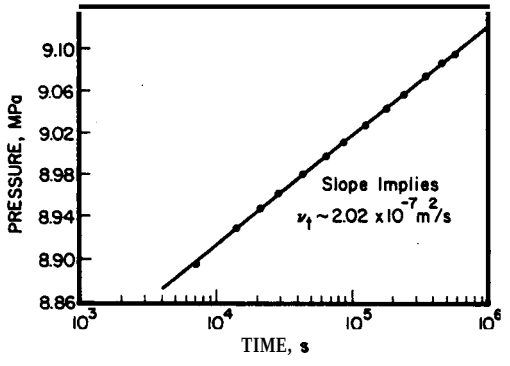

Figure 2 Pressure Injection Data for Case 2.

($\nu \sim 1.96 \times 10^{-7}$ m^2/s). Figures 3 and 4 show the radial distribution of steam saturation and temperature at the end of the injection period ($t = 5.868 \times 10^5$ s). The condensation front (especially in the low steam saturation case 2) is seen to have advanced further into the formation than the

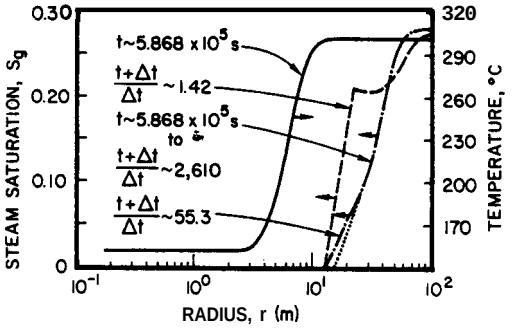

Figure 3 Radial Distribution of Temperature and Steam Saturation at Selected Times for Case 1.

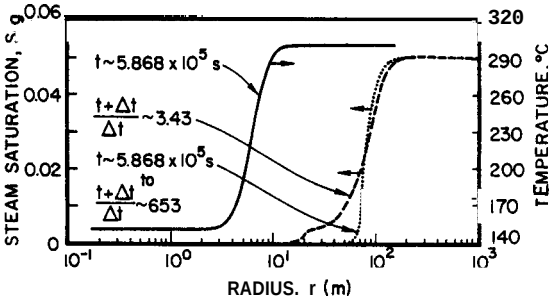

Figure 4 Radial Distribution of Temperature and Steam Saturation at Selected Times for Case 2.

edge of the thermal front. The latter effect is due to the fact that pressure changes are experienced over a much larger portion of tne reservoir than that which was cooled by the injected cold water.

Pressure Fall-Off Response Horner plots of pressure fall-off data are given in Fiqures 5 and 6. Tnree regions can be identified on these plots:

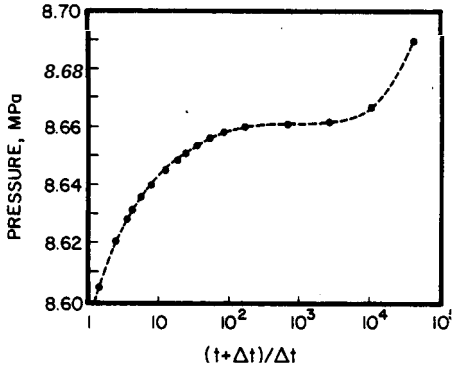

Figure 5 Pressure Fall-Off Data (Horner Plot) for Case 1.

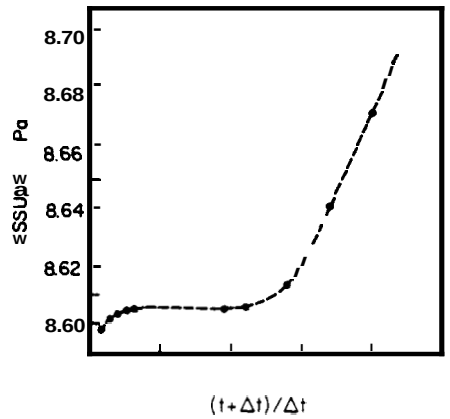

Figure 6 Pressure Fall-Off Data (Horner Plot) for Case 2.

(i) for large $(t + \Delta t)/\Delta t$ (i.e., small shutin times), pressure falls off relatively rapidly

(ii) for moderate values of $(t + \Delta t)/\Delta t$, pressure is essentially constant

(iii) for small values of $(t + \Delta t)/\Delta t$ (i.e., large buildup times), pressure again starts to fall rather rapidly.

The first region (i.e., $(t + \Delta t)/\Delta t$ large) of the fall-off curve is governed by the pressure response of the condensed fluid region. Due to the large contrast in single-phase and two-phase compressibilities, the two-phase region remains practically unaffected during this time period (see e.g., steam saturation profiles in Figures 3 and 4). The condensed fluid region behaves like a reservoir with a constant pressure (= pressure at the edge of the condensation front) boundary. These early pressure fall-off data are replotted in Figures 7 and 8; these figures clearly demonstrate that the early fall-off behavior in the present cases resembles that of a reservoir with a constant pressure boundary. The condensation front radius, r_e, can, therefore, be calculated from the formula (Earlougher [1977]):

$$r_e = \left(\frac{k \Delta t_s}{1.25 \phi \mu C_T} \right)^{0.5} \qquad (1)$$

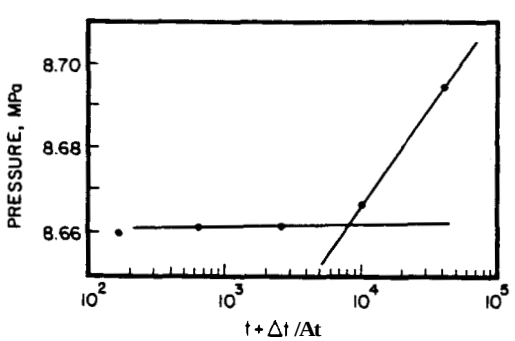

Figure 7 Early Pressure Fall-Off Data for Case 1.

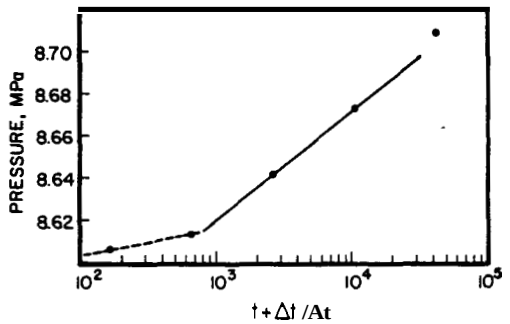

Figure 8 Early Pressure Fall-Off Data for Case 2.

where

k = formation permeability
Δt_s = time to startup of semi-steady reservoir behavior (time at which pressure curve bends over)
μ = viscosity of injected liquid water
C_T = Total formation compressibility in the condensed region.

The condensation front radii inferred from Equation (1) and the data of Figures 7 and 8 are compared with the actual values in Table 3.

Table 3
CONDENSATION FRONT RADII
($\mu = 1.8 \times 10^{-4}$ Pa-s; $C_T = 0.075 \times 10^{-8}$ Pa^{-1})

Case No	Δt_s	r_e (inferred)	r_e (actual)
1	72 s	14.6 m	(15.5 ± 1.5) m
2	753 s	47.2 m	(57.1 ± 5.2) m

Although the inferred values for r_e are in reasonable agreement with the actual values, a note of caution is in order here. In practical situations, the early fall-off data (such as that utilized in the above calculation for r_e) are liable to be dominated by wellbore storage, and it may well be impossible to identify the time at which the well starts exhibiting "semi-steady" response.

An examination of the numerical results snows that at the end of the first part of the fall-off curve, the pressure gradient in the single-phase (condensed) region is essentially zero whereas the pressure at the edge of the condensation front remains at its value at $\Delta t = 0$ (start of shutin period). Also, the edge of the condensation front is stationary throughout this initial period (Figures 3 and 4 - See steam saturation profiles for $t = 5.868 \times 10^5$ s to $(t + \Delta t)/\Delta t$ - (2610 in Figure 3, and 653 in Figure 4)).

During the intermediate fall-off period, the condensation front starts moving towards the wellbore. This part of the well response is cnaracterized by an essentially constant pressure. At the end of this period, the condensation front becomes coincident with the edge of the thermal front (see e.g., steam saturation curve labeled $(t + \Delta t)/\Delta t$ = 3.43 in Figure 4). The condensation front once again becomes stationary at this point.

For large fall-off times (i.e., for the third fall-off period), the well response is governed by the two-phase region. As can be seen from Figures 5 and 6, the pressure fall-off data do not, however, asymptote to a straight line. It is convenient to plot the fall-off data in a somewhat different manner. Figures 9 and 10 are plots of log Δp ($\Delta p = p_w(\Delta t) - p_f$ where p_f is the last flowing pressure) versus log Δt. Referring to Figure 10, it may be seen that the two-phase fall-off data lie on the unit slope line. A unit slope line can also be identified on Figure 9. It is well known that the presence of a unit slope line indicates that the well response is controlled by storage type effects; this part of the fall-off data is useless for analysis purposes in the absence of data regarding the location of tne condensation front (~ effective well-bore radius for two-phase fall-off regime). For single-phase flow, a rough rule of thumb is that the semi-log straight line starts at a time which is one and one-half log cycles removed from the time at which the pressure data begin to deviate from the unit slope straight line. Utilizing the latter criterion, it is seen from Figure 9 that only the last point or two may be expected to lie on the semi-log line. In view of the non-linear nature of two-phase flow in porous media, especially prior to the start of semi-log straight line, it would very likely be futile to try to analyze tne two-phase fall-off data of Figure 9 to derive kinematic mobility.

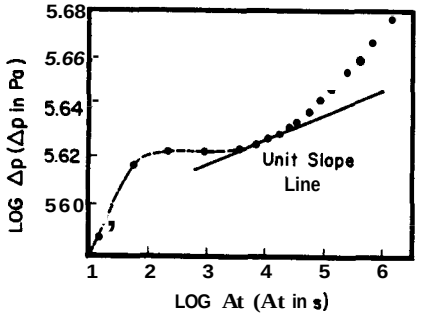

Figure 9 Plot of Log Δp Versus Log Δt for Case 1. ($\Delta p = p_w - p_f$; p_w is the well pressure at Δt and p_f is the last flowing pressure.) Note tnat the Vertical and Horizontal Scales are Different.

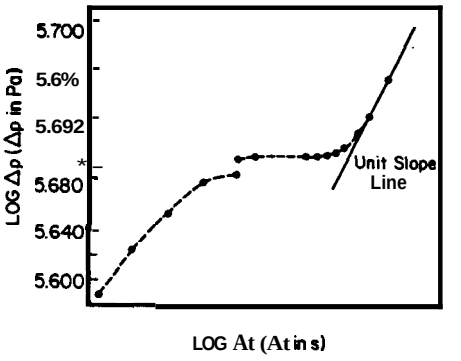

Figure 10 Plot of Log Δp Versus Log Δt for Case 2. ($\Delta p = p_w - p_f$; p_w is the well pressure at Δt and p_f is the last flowing pressure.) Note that (1) the Vertical and Horizontal Scales are Different, and (2) the Vertical Scale is Discontinuous.

Acknowledgment

Work performed under subcontract to WESTEC Services, Inc. with funding provided by the U. S. Department of Energy Under cooperative Agreement No. DE-FC03-78ET27163.

References

EARLOUGHER, R. C., Jr. [1977], Advances in Well Test Analysis, Monograph Series, Vol. 5, Society of Petroleum Engineers, Dallas, TX.

GARG, S. K. [1980], "Pressure Transient Analysis for Two-Phase (Water/Steam) Geothermal Reservoirs," SPEJ, pp. 206-214, June.

GRANT, M. A. [1978], "Two-Phase Linear Geothermal Pressure Transients: A Comparison With Single-phase Transients," New Zealand J. Sci., Vol. 21, pp. 355-364.

MOENCH, A. F. and P. G. Atkinson [1977], "Transient Pressure Analysis in Geothermal Steam Reservoirs With an Immobile Vaporizing Liquid Phase - Summary Report," Proc. Third Stanford Workshop on Geothermal Reservoir Engineering, Stanford, CA, pp. 64-69.

PRITCHETT, J.W. [1980], "Geothermal Reservoir Engineering Computer Code Comparison and Validation Calculations Using MSHM and CHARGR Geothermal Reservoir Simulators," Systems, Science and Software Report SSS-R-81-4749, November.

SOREY, M. L., M. A. Grant and E. Bradford [1980], "Nonlinear Effects in Two-Phase Flow to Wells in Geothermal Reservoirs," Water Resources Research, August.